Broadband Transponder Based on Frequency-Reconfigurable Cluster Antenna and Phased Modulators

Tauseef Ahmad Siddiqui [ID], Prabhat Khanal, Jari Holopainen [ID], and Ville Viikari [ID], *Senior Member, IEEE*

Abstract—This letter presents a new concept of broadband transponder based on frequency-reconfigurable cluster antenna and phase-variable modulators. The transponder in this concept has multiport antenna, whose elements have strong mutual coupling between them. The technique presented in this concept takes advantage of the coupling between the antenna elements instead of avoiding it. By properly weighting the phases of the modulated signals in each port, the backscattered received power can be maximized. The weighting is done differently for different sets of frequencies to achieve instantaneous bandwidth over the frequency band of interest.

Index Terms—Backscattering, impedance matching, Internet of Things (IoT), mutual coupling, modulation, scattering matrices, wireless sensor networks (WSNs).

I. Introduction

AMBIENT backscatter communication has been introduced as an emerging technology that enables smart devices [Internet of Things (IoT), wireless sensor networks (WSNs)] to communicate by utilizing available RF sources, e.g., TV towers, FM broadcasting stations, cellular base stations, and Wi-Fi access points [1]. The advantage of such ambient backscatter communication systems is that they do not require a dedicated frequency spectrum, which is scarce and costly. Another advantage is that there is no need to deploy dedicated radio frequency (RF) sources for backscatter devices.

The demand of increased data rates in smart devices require new techniques in antenna design. In order to fully utilize the available ambient RF energy in backscatter devices, the antenna needs to tune its operation to a frequency where the highest ambient power is available. This has led to the development of frequency-reconfigurable antennas, which apply a new strategy for getting proficient operation over a large frequency range. The antenna does not need to operate at all operating frequencies

simultaneously, making it possible to overcome the bandwidth requirements via frequency reconfigurability. Analog techniques have been deployed mainly to achieve the execution of frequency reconfigurable antennas, and these techniques change the electrical or physical length of the antennas [2]. Other solutions include matching networks with tunable capacitors [3], [4] and switchable matching networks [5], [6]. Both of these networks require separate matching networks for different frequency bands, and switching is required to select the matching network, leading to more space requirements on the printed circuit board (PCB) and an increase in losses in the system. The approach presented in our work exploits the digital part of the transceiver. Digital part generally takes smaller space in a PCB or integrated circuit (IC) chip compared to analog part, therefore, our approach might require less space. Furthermore, digital IC technology advances fast compared to analog components, where development is very modest.

Unlike the techniques in [2]–[6], frequency reconfiguration in [7] is done by using properly weighted incident signals at the antenna inputs. The theory presented in [7] is not applicable to transponders, and in this letter, for the first time we extend the concept for transponders. The theoretical approach in our case is novel and different from [7].

Current state-of-the-art transponders utilizing the modulated backscattering principle exhibit large modulated radar cross section at a narrow band. This is mainly because they rely on fixed antennas, whose impedance cannot be reconfigured. In the case of ambient rescattering operation principle, where the transponder captures an ambient wave, adds its own modulation to it, and redirects the modulated wave further, the frequency of the ambient wave is somewhat random. Broadband transponder in this scenario can utilize the ambient wave efficiently, whereas a fixed, narrowband transponder could utilize only certain spectral components.

This letter investigates broadband transponder implemented using frequency-reconfigurable cluster antenna. To the best of authors' knowledge, such transponders have not been presented previously. The suitability of the proposed approach is demonstrated by simulation and measurement results.

II. Theory

Fig. 1 illustrates the operation principle of broadband transponder. It is modeled by using multiple modulators, and
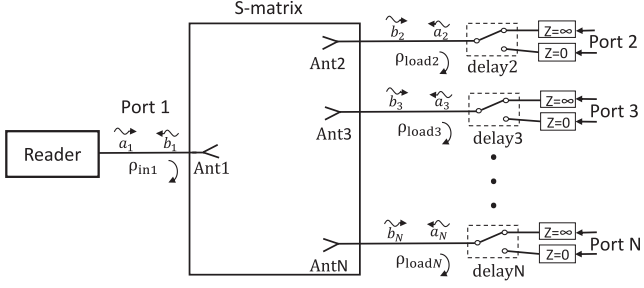
Fig. 1. Broadband transponder concept presented in this letter with *S*-parameter block and switchable loads. The transponder consists of multiple elements that have strong mutual coupling between them.
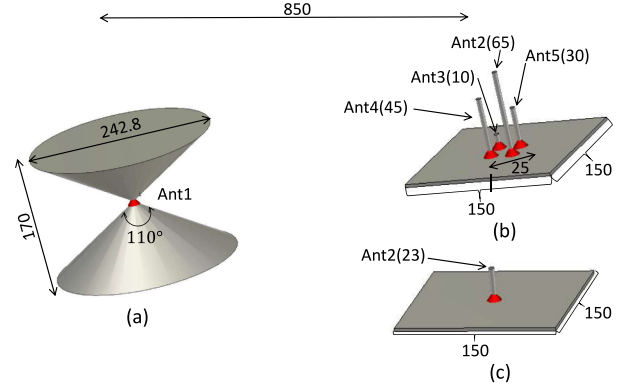

Fig. 2. (a) Reader antenna model. (b) Broadband studied transponder. (c) Reference narrowband transponder. All dimensions are in millimeters. The reader and transponder antennas are not to scale.

output of each modulator is connected to an antenna element. To create the phase difference between the outputs of the modulators, the switch-control signals of these modulators are delayed in the time domain. This is done because a delay in the time domain corresponds to a phase difference in the frequency domain. Switching the load between short and open circuits cause time-domain reflection coefficient $\rho(t)$ at the input of the switch that varies between $\rho_1 = -1$ and $\rho_2 = +1$, respectively. The modulated reflection coefficient at the input of the switch due to the changing loads in the frequency domain $\rho_{\text{load}}(\omega_m) = \rho_{\text{load}}$ is the Fourier transform of the time-domain reflection coefficient $\rho(t)$ over one period T. This is calculated as

$$\rho_{\text{load}} = \frac{-j}{2\pi} e^{-2jd\omega_m} \left(e^{jd\omega_m}(2\rho_1 - \rho_2) - \rho_2 \right) \quad (1)$$

in which $\omega_m = 2\pi f_m$, where $f_m = \frac{1}{T}$ is the modulation frequency and d is the time delay of the square signal used for modulation. Equation (1) gives the modulated reflection coefficient ρ_{load} at the first harmonic. The performance of the transponder in this letter is studied at the first harmonic only, hence (1) suffices to model the transponder.

Consider an *N*-port network as shown in Fig. 1 with reflection coefficients $\rho_{\text{load}j}$ at the loads, input reflection coefficient $\rho_{\text{in}1}$, and the scattering parameters S_{ij}. The input reflection coefficient at port 1 is

$$\rho_{\text{in}1} = \frac{b_1}{a_1} \quad (2)$$

and the load reflection coefficients at ports $2, 3, \ldots, N$ are

$$\rho_{\text{load}n} = \frac{a_n}{b_n}, \quad n = 2, \ldots, N. \quad (3)$$

Using (2) and (3), the scattering matrix can be rewritten as

$$\begin{bmatrix} b_1 \\ b_2 \\ \vdots \\ b_N \end{bmatrix} = \begin{bmatrix} S_{11} & S_{12} & \ldots & S_{1N} \\ S_{21} & S_{22} & \ldots & S_{2N} \\ \vdots & \vdots & \ddots & \vdots \\ S_{N1} & S_{N2} & \ldots & S_{NN} \end{bmatrix} \begin{bmatrix} b_1/\rho_{\text{in}1} \\ b_2\rho_{\text{load}2} \\ \vdots \\ b_N\rho_{\text{load}N} \end{bmatrix}. \quad (4)$$

For a transponder to function, we must have $\mathbf{b} \neq \mathbf{0}$ (port 1 is neither perfectly matched nor isolated). S_{11} is the reflection coefficient of the reader antenna, and it must be subtracted from the input reflection coefficient to get the modulated reflection coefficient. Therefore, by solving (4), the modulated reflection

coefficient ($\delta\rho_{\text{in}1}$) at port 1, when transponder have four coupled antenna elements, i.e., $N = 5$ can be written [9] as

$$\delta\rho_{\text{in}1} = \frac{-S_{21}D_2 + S_{31}D_3 - \cdots .. + S_{51}D_5}{D_1} \quad (5)$$

where D_N are the determinants of the minors, obtained of the matrix $(\mathbf{A} - \mathbf{I})^H$. The modulated reflection coefficient $\delta\rho_{\text{in}1}$ is defined as the ratio of the backscattered modulated voltage waves at modulated frequency $f_1 + f_m$ to the transmitted voltage wave at frequency f_1. The modulated reflection coefficients for the studied and reference transponders are calculated using (5). The delay values of (5) are optimized numerically to give largest modulated reflection coefficient $\delta\rho_{\text{in}1}$ for a given frequency [11].

III. SIMULATIONS

A. Transponder Design

The broadband transponder is intended to operate over a large frequency range of 1–6 GHz. The antenna model used for the studied transponder, shown in Fig. 2(b), consists of four monopole antenna elements grouped together in a 2×2 array, such that they are spaced 25 mm diagonally. The thickness of the monopole antenna elements are 2 mm. The structure is similar to antenna array but each antenna element is resonating at different frequencies. Fig. 3 shows the reflection coefficients of reader antenna and four antenna elements as a function of frequency. The lengths of the monopoles and the diagonal spacing between them are chosen such that at least two of the monopoles are simultaneously moderately matched and the mutual coupling is strong enough. In that case, the condition becomes favorable for canceling out the reflections. In a case of too poor matching level or too low mutual coupling, such as below 1 GHz, the condition for canceling out the reflections cannot be created. In [15], the design rules of the elements for creating the optimal condition in a two-antenna system is studied, but in a multiantenna system the situation is not unambiguous and precise design rules for the optimal condition are not yet available. The antennas are selected such that their operational bands cover the frequency range from 1 to 6 GHz. The reader antenna in Fig. 2(a) is a finite biconical antenna [10]. The biconical antenna has a very large bandwidth, and it can illuminate the transponder antennas in the
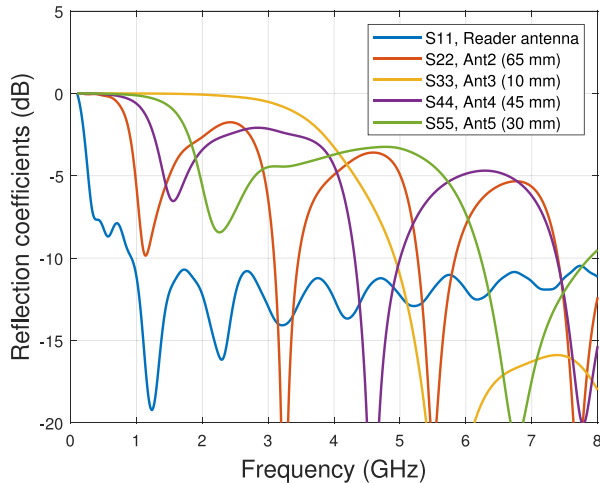
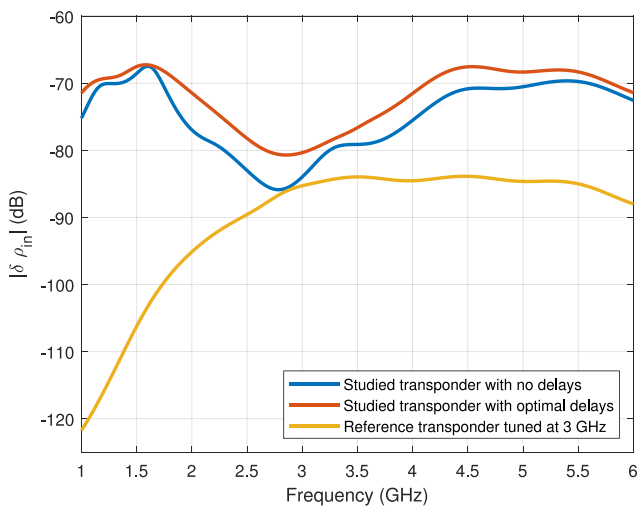Fig. 3.　Reflection coefficients as a function of frequency are shown.

Fig. 4.　Modulated received power, i.e., modulated reflection coefficient from (5) of the studied transponder and its comparison with reference transponder.

desired frequency range of 1 to 6 GHz. Both of these antenna models are modeled in CST Microwave Studio. The narrowband transponder shown in Fig. 2(c) is used as a reference, which is tuned at 3 GHz.

B. Simulation Results

Fig. 4 shows the received power at frequency $f_1 + f_m$ at the reader antenna when the transmitted power at frequency f_1 is 0 dBm (modulated received power in dBs at $f_1 + f_m = \delta\rho_{\text{in}1} +$ transmitted power). The simulation results show that the studied transponder performs better than reference transponder. In the best case at 1 GHz, the received power is more than 45 dB higher. The received power of the reference transponder near 3 GHz is large because its antenna is tuned at 3 GHz. Furthermore, the received power can be increased by using optimal delay values (see Fig. 4). These optimal delay values change as a function of frequency, and in the best case (e.g., at 2.8 GHz), the received power increases by even as much as 6 dB. The received power is low around 2.8 GHz when no delays are used because the impedance matching is poor at that frequency range. However,
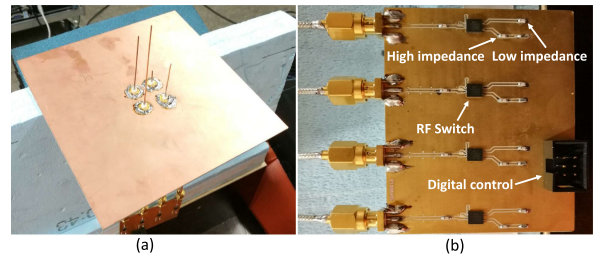

Fig. 5.　(a) Manufactured transponder prototype. (b) Modulator circuit.

when we use optimal delays, we can see maximum increment in the received power at 2.8 GHz (i.e., 6 dB). This result shows that the optimal delays can improve the impedance matching.

IV. Measurements

A. Transponder Prototype

The transponder prototype is made in order to demonstrate the behavior in real environment. We manufactured the prototype based on our simulated design. Fig. 5 shows the manufactured transponder prototype along with four modulators. The dimensions of these antenna elements are same as shown in Fig. 2. The SPDT RF switches (VSWA2-63DR+) are from mini-circuits. The input and output of the switches are connected to dc block capacitors of 47 pF. The switch inputs (RF-COM) are connected through SubMiniature version A (SMA) connectors to the antenna elements of the transponder. The switch outputs are connected to 2 MΩ resistor for high-impedance termination (open circuit), and to the ground directly for low-impedance termination (short circuit). The capacitors and resistors are from Murata. Earlier in this letter it was assumed that the modulator has ideal short and open circuits ($|\delta\rho| = |\rho_1 - \rho_2| = 2$), but in practice the situation is not ideal. However, the theory can be generalized for any load impedances. The load impedances of the prototype modulator were measured with the vector network analyzer and it was noticed that $|\rho_1 - \rho_2|$ is sufficiently large (mainly between 1 and 1.6) across the desired frequency range.

B. Measurement Setup

The measurements are performed in the anechoic chamber of School of Electrical Engineering, Aalto University, Espoo, Finland. Fig. 6 shows the measurement setup. It consists of a signal generator (R&S SML-03), spectrum analyzer (HP 8569E), logic analyzer (Agilent 16902 A), and transmitting (Tx) and receiving (Rx) antennas (ETS Lindgren 3164-08 quad-ridged horn antennas). From the signal generator, a transmit power of +24 dBm is applied at the frequency range of 1 to 6 GHz. The distance of the transponder from the Tx and Rx antennas is 1.6 m. The logic analyzer is used to create the necessary switch control signals for the modulators in the transponder. The transponder receives the signal transmitted by the reader antenna (Tx) and backscatters a modulated signal that is picked up with the other reader antenna (Rx) and detected with the spectrum analyzer.

The rise and fall time of RF switch is 23 ns. The logic analyzer produces square wave signal of 1 MHz whose rise and fall time is 5 ns, which is smaller than the rise and fall time of
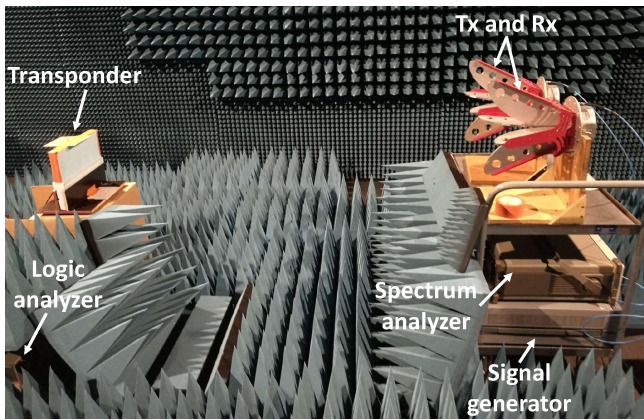
Fig. 6. Measurement setup used in the anechoic chamber. The distance (1.6 m) from the transponder to the Tx and Rx antennas is same.

RF switch used in the modulator. The logic analyzer generates four switch control signals for four modulators, which can be delayed by the resolution of 100 ns. When 1 MHz switch control signal is delayed with resolution of 100 ns, there are 10 different possible delay values. The switch control signal of the modulator connected to port 2 is taken as reference and its delay value is set to 0 in logic analyzer. The switch control signals of the modulators connected to ports 3, 4, and 5 are delayed with the resolution of 100 ns. There are 1000 different combinations of delay values. In this work, the measurements are done manually, and going through all 1000 different combinations are impractical. Therefore, five sets of arbitrary delay values are selected, and the measurements are done with these arbitrary delay sets. One arbitrary delay set consists of four delay values.

C. Measurement Results and Observations

The main difference in simulation and measurement setup is the far-field distance and Tx/Rx antennas are different therefore, there is no direct comparison between simulation and measurement results. However, the studied transponder is same in both setups, only the received power levels are different and general shape of the curve is comparable. The received power of the reference and studied transponders without delays is shown in Fig. 7. The measurement results show that the studied transponder performs better than the reference transponder except at 3 GHz because it is tuned at that frequency. The studied transponder performs up to 40 dB better than the reference transponder for instance at 1.1 GHz. These observations are similar to simulation results.

Fig. 8 shows the effect of delaying as a function of frequency with five arbitrary delay sets. The results show that delaying affects the received power quite a lot at most of the frequencies. At most, the effect is even more than 10 dB at 3.5 GHz. On the other hand, there are some frequencies where the arbitrary delaying does not have much effect, for instance, at 4 GHz the effect is only 3 dB. The possible reason may be related to the S-parameters, having nonoptimal matching and mutual coupling level at those frequencies. Also, the arbitrary delay distribution might not be optimal in those frequencies. The received power has increased at some frequencies and the best
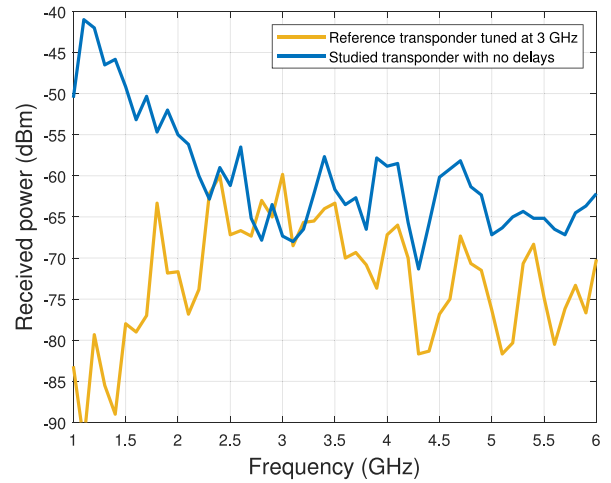

Fig. 7. Comparison of studied broadband transponder with no delays and with the reference transponder tuned at 3 GHz.
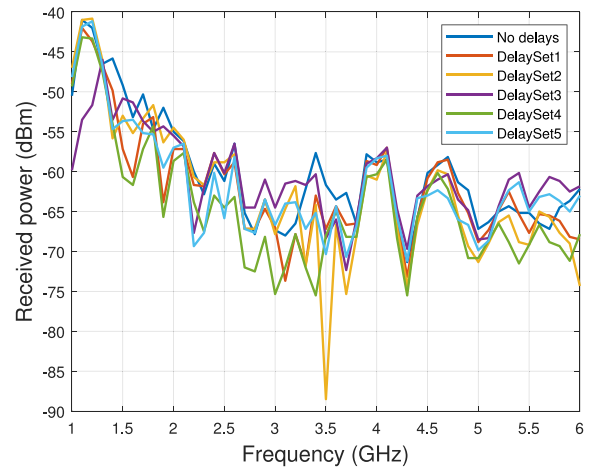

Fig. 8. Comparison of studied broadband transponder with no delays and with the five arbitrary delay sets.

value is of 6 dB increment we get at 5.7 GHz as compared to no delays. The measurement results prove that even with five arbitrary delay sets, the performance of the studied transponder has improved. The future directions of this work is to develop method for finding the optimal delay distribution for maximizing the received power.

V. CONCLUSION

In this letter, we presented a novel concept of a broadband transponder based on the frequency reconfigurability of its antenna. The simulation and measurement results show that delaying the modulators significantly affects the received power performance of the proposed transponder. More research is required in finding the solutions to implement optimal delay distribution. We can get higher received power but it also depends on how complex it is to implement the optimal delay system in real practice. The antenna research questions also include, e.g., how the resonance frequencies and coupling should be designed in a multiport system to cancel the reflections.

REFERENCES

[1] N. Van Huynh, D. T. Hoang, X. Lu, D. Niyato, P. Wang, and D. I. Kim, "Ambient backscatter communications: A contemporary survey," *IEEE Commun. Surveys Tuts.*, vol. 20, no. 4, pp. 2889–2922, Oct.–Dec. 2018.

[2] R. M. C. Cleetus and G. J. Bala, "Frequency reconfigurable antennas: A review," in *Proc. Int. Conf. Signal Process. Commun.*, Jul. 2017, pp. 160–164.

[3] J. Ilvonen, R. Valkonen, J. Holopainen, and V. Viikari, "Multiband frequency reconfigurable 4 G handset antenna with MIMO capability," *Prog. Electromagn. Res.*, vol. 148, pp. 233–243, 2014.

[4] S. Caporal Del Barrio, A. Tatomirescu, G. Pedersen, and A. Morris, "Novel architecture for LTE world-phones," *IEEE Antennas Wireless Propag. Lett.*, vol. 12, pp. 1676–1679, 2013.

[5] R. Valkonen, C. Luxey, J. Holopainen, C. Icheln, and P. Vainikainen, "Frequency-reconfigurable mobile terminal antenna with MEMS switches," in *Proc. 4th Eur. Conf. Antennas Propag.*, Barcelona, Spain, Apr. 2010, pp. 1–5.

[6] R. Valkonen, J. Holopainen, C. Icheln, and P. Vainikainen, "Broadband tuning of mobile terminal antennas," in *Proc. 2nd Eur. Conf. Antennas Propag.*, Nov. 2007, pp. 1–6.

[7] J.-M. Hannula, J. Holopainen, and V. Viikari, "Concept for frequency reconfigurable antenna based on distributed transceivers," *IEEE Antennas Wireless Propag. Lett.*, vol. 16, pp. 764–767, 2017.

[8] G. B. Arfken and H. J. Weber, *Mathematical Methods for Physicists International Student Edition* (Fourier series). Amsterdam, The Netherlands: Elsevier, 6th ed., ch. 14, p. 881, 2005.

[9] J. X. Yun and R. G. Vaughan, "A view of the input reflection coefficient of the n-port network model for MIMO antennas," in *Proc. IEEE Int. Symp. Antennas Propag.*, Jul. 2011, pp. 297–300.

[10] W. L. Stutzman and G. A. Thiele, "Biconical antenna" in *Antenna Theory and Design*, 3rd ed. Hoboken, NJ, USA: Wiley, ch. 7.4, pp. 233–239, 2012.

[11] Wolfarm Research, "Wolfarm Mathematica 11," 2019. [Online]. Available: http://www.wolfram.com/mathematica/

[12] J.-M. Hannula, T. Saarinen, J. Holopainen, and V. Viikari, "Frequency reconfigurable multiband handset antenna based on a multichannel transceiver," *IEEE Trans. Antennas Propag.*, vol. 65, no. 9, pp. 4452–4460, Sep. 2017.

[13] J.-M. Hannula, T. O. Saarinen, A. Lehtovuori, J. Holopainen, and V. Viikari, "Tunable eight-element MIMO antenna based on the antenna cluster concept," *Microw., Antennas Propag.*, vol. 13, no. 7, pp. 959–965, Dec. 6, 2019. [Online]. Available: https://digital-library.theiet.org/content/journals/10.1049/ietmap.2018.5742

[14] J.-M. Hannula *et al.*, "Performance analysis of frequency-reconfigurable antenna cluster with integrated radio transceivers," *IEEE Antennas Wireless Propag. Lett.*, vol. 17, no. 5, pp. 756–759, May 2018.

[15] J.-M. Hannula, A. Lehtovuori, R. Luomaniemi, T. O. Saarinen, and V. Viikari, "Beneficial interaction of coupling and mismatch in a two-antenna system," in *Proc. 13th Eur. Conf. Antennas Propag.*, Krakow, Poland, Mar.–Apr. 2019.